A Southern Hemisphere VLBI Survey on a 275-km Baseline

D. D. Morabito, R. A. Preston, J. Faulkner, and A. E. Wehrle
Tracking Systems and Applications Section

D. L. Jauncey, M. J. Batty, R. F. Haynes, and A. E. Wright
C.S.I.R.O., Division of Radiophysics, Epping, Australia

A VLBI survey at 2.29 GHz has been conducted using a 275-km baseline consisting of the NASA DSN tracking site in Tidbinbilla, Australia, and the 64-m antenna located at Parkes, Australia. The purpose of this survey was to identify sources in the southern sky possessing strong compact cores (< 0.1 arcseconds). Such sources will be used to form a reference frame for conducting VLBI geodesy experiments in the southern hemisphere. The 70 candidate sources were chosen to be south of -39 degrees declination, and only four had been previously observed from the northern hemisphere. Of the observed sources, 49 were found to have compact structure. In addition to determining correlated flux densities, the delay and delay rate observables of several detected sources were used to determine an estimate of the three-dimensional location of the Parkes antenna relative to the Tidbinbilla site with a 1-sigma accuracy of < 10 meters.

I. Introduction

Prior to April 1980, there had been very few sources observed with VLBI in the southern polar region due to the dearth of antennas in the southern hemisphere with built-in VLBI capabilities. From 24-28 April 1980 a VLBI experiment at 2.29 GHz was performed between the NASA DSN site at Tidbinbilla, Australia, and the 64-m antenna at Parkes, Australia, for the purpose of identifying sources possessing compact components and hence useful for southern hemisphere VLBI geodesy experiments. This paper discusses the results of that survey.

The candidate sources were selected from the Parkes survey (Refs. 1-10). The selection criteria were (1) catalog total flux density > 1.0 Jy at 2.7 GHz, (2) spectral index >-0.7 ($S=kf^{\alpha}$), and (3) declination south of -39 degrees. Of 95 sources meeting these criteria, 70 sources were observed. Of these sources, 49 were found to have a compact core on the Tidbinbilla to Parkes baseline (~0.1 arcsec fringe spacing). Selected sources from these 49 new VLBI detections combined with sources previously detected by VLBI (mostly with declinations north of -39 degrees) (Ref. 11), and sources detected in future VLBI surveys will be used to construct a celestial reference frame for performing southern hemisphere VLBI geodesy experiments. The advent of southern hemisphere VLBI will be of great value to both the geodynamic and astrophysics communities. The seismically quiet Australian continent will serve as a stable platform for testing long-term reliability and repeatability of VLBI-determined geodetic relative positions, and as a base for using VLBI to measure the crustal motions of the very seismically active regions near Australia.

II. Experiment Configuration

Right circular polarization was employed. The NRAO Mark II VLBI recording system was used to record a 1.8-MHz data bandwidth by digitally sampling at 4 Mbs (Ref. 12). Digital sampling and phase stability of the receiver chain were controlled by a rubidium atomic oscillator at Parkes and a hydrogen maser at Tidbinbilla. Each source was observed for three minutes. The Tidbinbilla/Parkes interferometer has a length of 275 km, corresponding to a minimum fringe spacing of 98 milliarcsec at 2.29 GHz.

Total flux densities for most of the sources were measured during the experiment with the 64-m antennas at Parkes and Tidbinbilla. The rms errors were $[(0.05\,S)^2 + (0.03)^2]^{0.5}$ Jy for Tidbinbilla and $[(0.1\,S)^2 + (0.03)^2]^{0.5}$ Jy for Parkes, where S is the measured total flux density.

III. Data Reduction

Matching tapes from both sites were cross-correlated using the Caltech/JPL VLBI Block 0 Processor (Mark II). Computer manipulation of the correlator output yielded the correlation coefficient for each observation. The tapes were correlated over a range of relative tape delay and delay rate offsets to compensate for a priori source position uncertainties. The sky was searched within 2 arcmin of all a priori source positions.

The correlation coefficients were then converted into correlated flux densities or the VLBI source strength for each celestial radio source observation using the procedure discussed in a previous paper (Ref. 13) with a scaling constant of 2.5 ±0.1 Jy. The 5-sigma detection limit for each observation was about 0.1 Jy. Correspondingly, the uncertainty in detected source strength due to random noise was about 0.02 Jy. However, in practice, systematic errors at about the 7% level dominate the random contributions for most sources.

The delay and delay rate observables of 31 detected sources were used to solve for the DSS 42 to Parkes baseline. Most of the source positions used in this solution were determined from VLBI experiments between Australia and South Africa performed during the same week (Ref. 14). The rest of the positions were obtained from Fanselow et al. (Ref. 15). The delays were bit stream alignment delays yielding post-fit residuals of about 10 ns. Post-fit residuals in delay rates were about 0.5 mHz.

IV. Results and Discussion

Table 1 lists the total flux densities, the correlated flux densities, and the number of observations for each source. For cases where multiple observations of correlated flux density differ by more than 1 sigma (probably due to source structure effects), both the lowest value (denoted by L) and the highest value (denoted by H) are listed in the table. Undetected sources are denoted by 5-sigma upper bound.

Figure 1 shows a sky distribution plot of the detected sources. This plot along with the results given in Table 1 can serve as a useful tool in creating an optimum observing schedule for conducting VLBI geodesy experiments. Figure 2 shows a correlated flux density histogram of the detected sources. Note that there are 10 sources with mean flux densities greater than or equal to 2 Jy.

The baseline vector from DSS 42 to Parkes was determined as a by-product of this survey. By assuming the previously determined position of DSS 42 (Ref. 16), the new position of the Parkes antenna intersection of axes is

X = -4554229 m
Y = 2816762 m
Z = -3454050 m

where X is the vector component aligned along the Greenwich meridian on the equatorial plane, Y is the vector component aligned 90 degrees east of Greenwich on the equatorial plane, and Z is the vector component aligned along the earth's spin axis defined positive north. The 1-sigma accuracy of the baseline measurements is < 10 meters in each coordinate.

This result agrees with a recent ground survey (Ref. 17), but differs from the position published in the 1981 American Ephemeris by -140 m in X, 46 m in Y, and 133 m in Z. This solution is a fourteenfold improvement over the previously known Parkes antenna position.

V. Conclusion

A 2.29-GHz VLBI survey of 70 southern polar sources on a 275-km baseline found 49 of these sources to have compact cores. These sources will be useful for future VLBI geodesy experiments in the southern hemisphere. As a by-product of this survey, the position of the Parkes antenna was determined with a 1-sigma accuracy of < 10 meters.

Acknowledgments

We are indebted to the instrumentation and observing assistance supplied by L. J. Skjerve of JPL and to the staffs of the Tidbinbilla and Parkes observatories.

References

1. Shimmins, A.J., and Bolton, J.G., *Aust. J. Phys. Astrophys. Suppl.*, No. 26,1, 1972.
2. Bolton, J.G., and Butler, P.W., *Aust. J. Phys. Astrophys. Suppl.*, No. 34,33, 1975.
3. Wall, J.V., Shimmins, A.J., and Bolton, J.G., *Aust. J. Phys. Astrophys. Suppl.*, No. 34,55, 1975.
4. Wright, A.E., Savage, A., and Bolton, J.G., *Aust. J. Phys. Astrophys. Suppl.*, No. 41,1, 1977.
5. Shimmins, A.J., *Aust. J. Phys. Astrophys. Suppl.*, No. 21,1, 1971.
6. Bolton, J.G., and Shimmins, A.J., *Aust. J. Phys. Astrophys. Suppl.*, No. 30,1, 1973.
7. Ekers, J.A., *Aust. J. Phys. Astrophys. Suppl.*, No. 7,1, 1969.
8. Shimmins, A.J., Manchester, R.N., and Harris, B.J., *Aust. J. Phys. Astrophys. Suppl.*, No. 8,1, 1969.
9. Shimmins, A.J., and Bolton, J.G., *Aust. J. Phys. Astrophys. Suppl.*, No. 23,1, 1972.
10. Wills, B.J., *Aust. J. Phys. Astrophys. Suppl.*, No.. 38,1, 1975.
11. Preston, R.A., et al. (to be published in the *Astrophysical Journal*).
12. Clark, B.G., *Proc. IEEE*, 61,1242, 1973.
13. Preston, R.A., et al., *DSN Progress Report 42-46*, Jet Propulsion Laboratory, Pasadena, Calif., Aug. 15, 1978.
14. Morabito, D.D., et al., *Astronomical Journal* (in press).
15. Fanselow, J.L., et al. (private communication).
16. Moyer, T.D. (private communication).
17. Allman, J.S. (private communication) 1983.

Table 1. Table of observations

SOURCE NAME	TOTAL FLUX DENSITY (Jy)		CORRELATED FLUX DENSITY (Jy)	NUMBER OF OBSERVATIONS
P 0003-56	0.86+/- 0.09		<0.07	1
P 0003-42	1.3 +/- 0.1		0.15+/- 0.02	1
P 0036-62	0.79+/- 0.08		<0.07	1
P 0043-42	4.8 +/- 0.5		<0.07	1
P 0047-579	2.7 +/- 0.3		1.5 +/- 0.1	1
P 0131-522	1.4 +/- 0.1		0.96+/- 0.07	1
P 0153-410	1.6 +/- 0.2		1.21+/- 0.09	1
P 0202-76	1.9 +/- 0.2		0.28+/- 0.03	1
P 0208-512	3.5 +/- 0.4		2.3 +/- 0.2	1
P 0214-48	1.4 +/- 0.2		<0.07	1
P 0302-623	1.7 +/- 0.2		1.4 +/- 0.1	1
P 0332-403	1.2 +/- 0.07	L	0.66+/- 0.05	2
		H	1.28+/- 0.09	
P 0354-48	0.39+/- 0.05		<0.07	1
P 0427-53	3.5 +/- 0.4		<0.07	1
P 0437-454	0.71+/- 0.08		0.62+/- 0.05	1
P 0438-43	3.9 +/- 0.2	L	2.3 +/- 0.2	2
		H	3.2 +/- 0.2	
P 0454-46	2.1 +/- 0.2		1.30+/- 0.09	1
P 0506-61	1.8 +/- 0.2		<0.07	1
P 0511-48	2.5 +/- 0.3		<0.07	1
P 0514-459			0.72+/- 0.05	1
P 0517-56	1.0 +/- 0.1		<0.07	1
P 0535-66	1.2 +/- 0.1		<0.07	1
P 0537-441	3.3 +/- 0.3		2.6 +/- 0.2	1
P 0616-48	0.66+/- 0.07		<0.07	1
P 0637-75	5.1 +/- 0.5		3.6 +/- 0.3	1
P 0658-65	0.86+/- 0.09		<0.07	1
P 0719-55	1.2 +/- 0.1		<0.07	1
P 0743-67	3.0 +/- 0.3		1.15+/- 0.08	1
P 0748-44	1.4 +/- 0.1		<0.07	1
P 0842-75	2.6 +/- 0.3		0.14+/- 0.02	1
P 0903-57	1.7 +/- 0.2		0.11+/- 0.02	1
P 1046-409	1.8 +/- 0.2		0.52+/- 0.04	1
P 1104-445	2.1 +/- 0.2		1.8 +/- 0.1	2
P 1105-680			0.75+/- 0.05	1
P 1148-671			1.6 +/- 0.1	1
P 1215-45	3.7 +/- 0.4		2.0 +/- 0.1	1

SOURCE NAME	TOTAL FLUX DENSITY (Jy)		CORRELATED FLUX DENSITY (Jy)	NUMBER OF OBSERVATIONS
P 1302-49	4.9 +/- 0.3		<0.08	1
P 1416-49	1.63+/- 0.09		0.09+/- 0.01	1
P 1421-49	7.4 +/- 0.4	L	1.7 +/- 0.1	6
		H	3.3 +/- 0.2	
P 1424-41	2.6 +/- 0.1	L	1.4 +/- 0.1	8
		H	1.8 +/- 0.1	
P 1540-82	1.20+/- 0.07		1.12+/- 0.09	1
P 1549-79	5.4 +/- 0.3	L	2.5 +/- 0.2	2
		H	3.0 +/- 0.2	
P 1602-63	2.2 +/- 0.1		0.05+/- 0.01	1
P 1610-77	4.4 +/- 0.2		3.7 +/- 0.2	2
P 1619-680	1.8 +/- 0.1		1.9 +/- 0.1	5
P 1637-77	4.3 +/- 0.2		0.14+/- 0.01	1
P 1655-77	1.74+/- 0.09		<0.04	1
P 1718-649	4.2 +/- 0.2		3.8 +/- 0.2	2
P 1733-56	5.8 +/- 0.3		1.18+/- 0.06	2
P 1806-458	1.26+/- 0.07		0.43+/- 0.02	2
P 1815-554	1.12+/- 0.06		1.06+/- 0.08	1
P 1831-711	1.12+/- 0.06		0.85+/- 0.06	1
P 1933-58	1.9 +/- 0.1		0.31+/- 0.02	2
P 1936-623	1.37+/- 0.07		0.86+/- 0.05	2
P 1951-50	0.94+/- 0.06		<0.07	2
P 2002-50			0.24+/- 0.02	1
P 2005-489			0.96+/- 0.07	1
P 2052-47			1.26+/- 0.06	2
P 2106-413			1.8 +/-0.1	2
P 2153-69	20.8 +/- 2.1		0.75+/- 0.05	1
P 2204-54	1.09+/- 0.1		<0.07	1
P 2207-45			<0.07	1
P 2213-45			0.69+/- 0.05	1
P 2227-399	0.41+/- 0.05		0.53+/- 0.04	1
P 2311-452	2.0 +/- 0.2		1.4 +/- 0.1	1
P 2326-477	2.8 +/- 0.3		2.4 +/- 0.2	2
P 2333-528	1.7 +/- 0.2		1.32+/- 0.09	1
P 2338-58	1.8 +/- 0.2		<0.07	1
P 2355-534			1.5 +/- 0.1	1
P 2356-61	16.9 +/- 1.7		<0.08	2

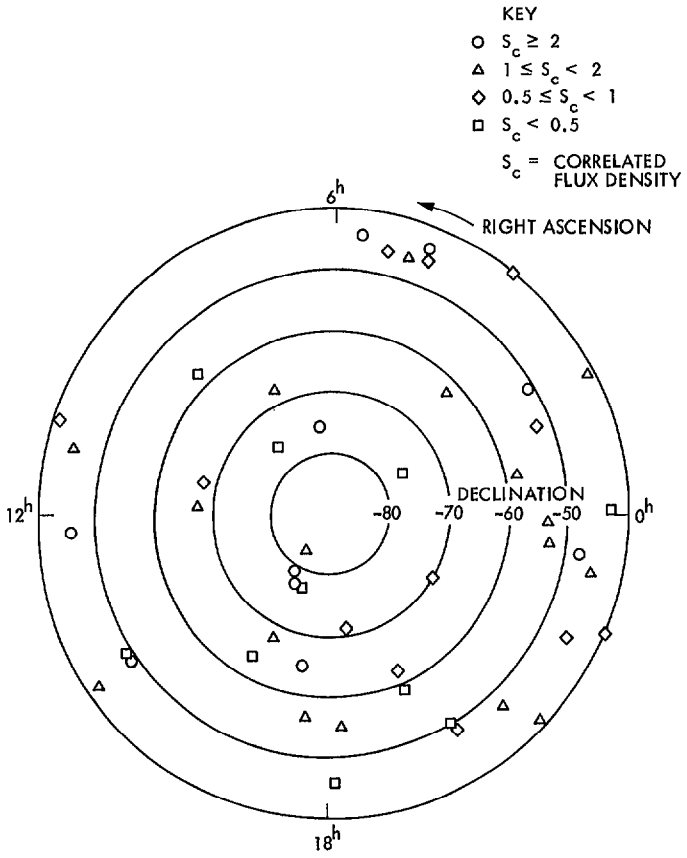

Fig. 1. Sky distribution plot

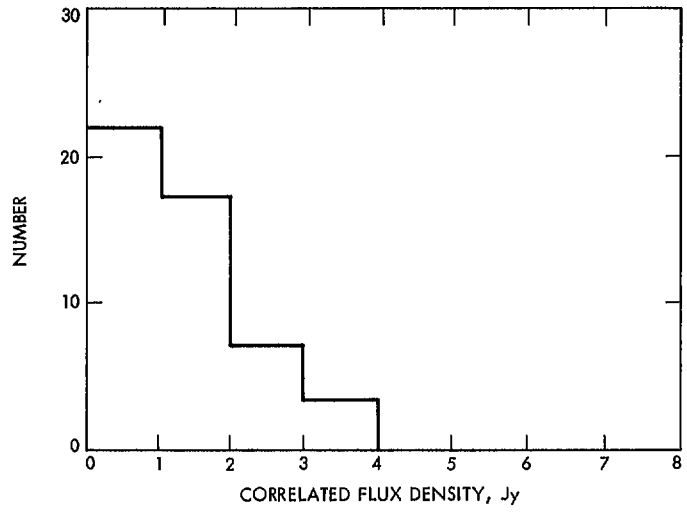

Fig. 2. Correlated flux density histogram